Journal of Molecular Structure 1320 (2025) 139701

Contents lists available at ScienceDirect

Journal of Molecular Structure

journal homepage: www.elsevier.com/locate/molstr

Structural and antibacterial assessment of two distinct dihydroxy biphenyls encapsulated with β-cyclodextrin supramolecular complex

Kumaraswamy Paramasivaganesh [a,c], Chandramohan Govindasamy [b], Esakkimuthu Shanmugasundaram [a], Nithesh Kumar Krishnan [a], Chokalingam Saravanan [d], Jayaraman Thanusu [e], Stalin Thambusamy [a,*]

[a] Department of Industrial Chemistry, Alagappa University, Karaikudi 630003, Tamil Nadu, India
[b] Department of Community Health Sciences, College of Applied Medical Sciences, King Saud University, P.O. Box 10219, Riyadh 11433, Saudi Arabia
[c] Department of Chemistry, Arumugam Pillai Seethai Ammal College, Tiruppattur 630211, Tamil Nadu, India
[d] Department of Chemistry, CHRIST (Deemed to be University), Bangalore 560029, Karnataka, India
[e] Department of Chemistry, Alpha College of Engineering, Chennai 600124, Tamil Nadu, India

ARTICLE INFO

Keywords:
β-cyclodextrin
Inclusion complex
Optical studies
Solid inclusion complex
Antibacterial activity
Gram-positive and gram-negative bacteria

ABSTRACT

β-Cyclodextrin plays a vital role in biological application because it can enhance the stability and solubility of the guest molecules in the supramolecular inclusion complexes. Moreover, the β-Cyclodextrin inclusion complex has control-releasing behavior and lower toxicity than bare guest molecules. To improve the solubility and stability properties of two structurally different fluorescent guest molecules, namely 2,2′-dihydroxy biphenyl and 3,3′-dihydroxy biphenyls, they involve the β-Cyclodextrin inclusion complex process. Optical measurements clearly described the efficient binding through the changes in the absorbance and emission intensities of guest molecules in the presence of β-Cyclodextrin. The Job's plot from absorbance measurements reveals the 1:1 stochiometric ratio of binding of guests and the β-Cyclodextrin host. The FT-IR spectra of the solid complex show the characteristic stretching and bending vibrations from both the guests and the host molecule. The ^{1H}NMR spectra of the inclusion complex promote downfield shifting of guest molecule protons upon binding with the β-Cyclodextrin host. The solid complex prepared using the solution method exhibits superior antibacterial activity against both gram-positive and gram-negative bacteria compared to the kneading and physical mixing methods.

1. Introduction

Macrocycle-based supramolecular complex proposed numerous supramolecular building blocks through inter- and intramolecular non-covalent interactions (hydrogen bonding, hydrophobic interactions, electrostatic, and π-π interactions) with widespread applications in the branches of chemical, material, pharmaceutical, and biological sciences [1–4]. Macrocyclic supramolecular compounds such as Crown ethers, Cyclodextrins, Calix [n]arenes, Pillar [n]arenes, and Cucurbit [n]urils offer confined and rigid or flexible cavities to accommodate biologically or industrially important smaller-size molecules [5–8]. The upper and lower rim functionalized macrocycles create greater influence towards the selective recognition and sensitive detection of lots of drugs, pesticides, heavy metal ions, and dye molecules [9–12].

Cyclodextrins (CDs) are bucket-shaped cyclic oligosaccharides composed of glucopyranose units with different cavity sizes categorized as α-cyclodextrin ($n = 6$), β-cyclodextrin ($n = 7$) and γ-cyclodextrin ($n = 8$) [13–15]. Which provides a hydrophobic inner and hydrophilic outer cavity that acts as a carrier or host to attract polar and non-polar guest molecules to form a stable host-guest complex [11,16–18]. CDs are claimed to be a safer host molecule to encapsulate pharmaceutical molecules and raise the guest properties such as rate of dissolution, greater stability, suppressed bad odour and volatility, prevent oxidation and light-induced side reactions [19,20]. Inclusion complexation of seven-membered β-cyclodextrin host with a variety of biologically important guest molecules such as vitamins, [21], antibiotics [22–24], painkillers [25], essential oils [26] and phenolic compounds [27,28] has been contributed gratefully to the medical and food industry. Tang et. al., (2015) described the enhancement in the solubility and dissolution of poorly soluble chlorzoxazone drug through β-cyclodextrin inclusion [29]. Chatzidaki et.al., (2020) evaluated the pharmacophore structures and antioxidant efficiency of two synthetic antioxidants in the presence

* Corresponding author.
E-mail address: stalin.t@alagappauniversity.ac.in (S. Thambusamy).

https://doi.org/10.1016/j.molstruc.2024.139701
Received 16 May 2024; Received in revised form 7 August 2024; Accepted 18 August 2024
Available online 19 August 2024

of β-cyclodextrin [30]. Srinivasan et.al., (2014) analysed the photophysical properties and guest binding characteristics of some dinitro derivatives of phenol, aniline, and benzoic acid upon incorporation into the β-cyclodextrin host cavity [31,32]. Mohandoss et.al., (2015), have established several host-guest systems of β-cyclodextrin with anthraquinone derivatives such as 1,2dihydroxyanthraquinones, 1,4dihydroxylanthraquinone,1,5dihydroxylanthraquinone as fluorescent guest molecules with huge biological importance and as chemo sensor [14,33].

The supramolecular complex contains bioactive quinoxaline-1,4-dioxide incorporated into a β-cyclodextrin derivative has delivered outstanding antibacterial activity against multiple bacterial strains [34]. Caffeic acid/cyclodextrins inclusion complex associated with poly (vinyl alcohol) electrospun nanofibers showed high antibacterial efficacy against Escherichia coli and Staphylococcus aureus [35]. Hydroxybiphenyls and substituted hydroxybiphenyls are the key intermediates derived from the microbial metabolism of dibenzofuran, fluorene, and carbazole, which are applied as antioxidants in foodstuffs and oil additives [5,36]. Our previous work also deals with the structural investigation and antibacterial assessment of biphenyl-3,3′,4,4′-tetraamine and 4,4′-diaminobiphenyl-3,3′-diol/β-cyclodextrin inclusion complex [37]. Reports on the biological activity of dihydroxybiphenyl derivatives are limited, and their potential medicinal properties are unexplored. Dihydroxybiphenyl has a higher antioxidant property and biologically active nature due to the hydroxyl groups presented in their benzene rings. The hydroxyl groups can improve the generation of reactive oxygen species (ROS) that induce oxidative stress and cellular damage (DNA, proteins, and lipids). The damage can promote cell death. Moreover, the hydroxyl groups easily interact with the cell membrane by the hydrogen bonds and destroy the cells. Therefore, in the present investigation, the inclusion complex of 2,2′-dihydroxybiphenyl and 3,3′-dihydroxybiphenyl with β-cyclodextrin has been prepared, and its structural interactions were examined successfully in solution and as a solid complex. The intermolecular hydrogen bonding interactions could be the major induction for the host-guest binding between the guest and the host molecule. The antibacterial activity has been carried out on gram-positive and gram-negative bacteria using both the guest molecules and the inclusion complex.

2. Experimental section

2.1. Materials

β-Cyclodextrin was purchased from SD Fine Chemicals, Bengaluru, India, and used without further purification. 2,2′-dihydroxybiphenyl and 3,3′-dihydroxybiphenyl were obtained from Sigma-Aldrich Chemicals in India. Millipore water was used for the preparation of all stock and the sample solutions.

2.2. Instruments

UV–visible spectral titration measurements are executed using SCHIMADZU UV-2401 PC. Fluorescence spectral titrations are performed using the JASCO FP-8200 Spectrofluorometer. The FTIR spectra are measured in the range of 4000–400 cm^{-1} on a Jasco FTIR 4600 spectrometer using a KBr pellets press. Surface morphologies are studied using the FEI QUANTA 250 scanning electron microscope (SEM). The NMR spectral titrations are made using Bruker 500 MHz NMR Spectrometer.

2.3. Binding constant calculation from absorption and emission spectral titrations

The guest's 22-DHBP and 33-DHBP concentrations are fixed at 1×10^{-4} M and the β-CD concentration is varied from 1×10^{-3} M to 12×10^{-3} M and the absorption changes are recorded. The binding constant value is calculated from the changes in the absorption maxima of guest molecules using the Benesi-Hildebrand relation [38].

$$1/\Delta A = 1/K_a \Delta\varepsilon[H] + 1/\Delta e[G] \quad (1)$$

Where, ΔA - The changes in the absorbance of guests upon the addition of β-CD host. Δε - The difference between the molar extinction coefficient for the guest alone and β-CD complex. [H] - The total concentration of β-CD host. [G] - The total concentration of guests (22-DHBP and 33-DHBP). The plot of 1/ΔA vs. 1/ [G] showed a straight line. The binding constant K_a is calculated from the slope. The ratio of association of host and guest is calculated using Job's plot. The mixture is prepared using β-CD host (varied from 1×10^{-4} M to $12 \times 10^{-}4$ M) and guest (varied from 12×10^{-4} M to 1×10^{-4} M) and the absorption changes are measured. The Job's plot is made from a change in absorption with mole fraction and holds a stoichiometric ratio and the binding.

The binding constant value is determined from emission measurement using a modified Stern-Volmer equation [7,39].

$$log[(F_0 - -F)/F] = nlog[H] log K_a \quad (2)$$

Where F_0 is the fluorescence intensity of the guest, F is the fluorescence intensity of the guest in the presence of β-CD host, [H] is the concentration of β-CD, K_a is the binding constant, and n is the stoichiometric ratio of guest/host complex.

2.4. Preparation of solid inclusion complex of 22-DHBP and 33-DHBP with β-CD

About 1 g of accurately weighed β-CD was placed into a 100 mL beaker and 30 mL Millipore water was added and stirred. Then, 0.16 g of 2,2′-DHBP or 3,3′-DHBP was accurately weighed, transferred into a 50 ml beaker, and separately dissolved using 20 mL ethanol. The ethanolic solution of 22-DHBP or 33-DHBP solution was slowly poured into the stirred β-CD solution. Room temperature stirring was continued for 24 hrs. Afterward, the reaction mixture was kept in the refrigerator for 24 hrs. At that time, a white color product was formed. The resultant product was filtered and washed with Millipore water and ethanol and dried in an oven at 50 °C for 12 h. The obtained solid complex was used for further analysis.

2.5. Preparation of solid inclusion complex of 22-DHBP and 33-DHBP with β-CD from the **kneading method**

The 1:1 ratio of β-CD:22-DHBP or 33-DHBP was weighed and transferred into a mortar. Then, a small amount of water and ethanol should be added to the mixture and made into a paste. The mixtures in the motor should be grained for 1 hour and dried in an air oven at 50 °C for 12. The mixture should be transferred and stored in an airtight container.

2.6. Preparation of solid inclusion complex of 22-DHBP and 33-DHBP with β-CD from the physical mixture method

In this method, the 1:1 ratio of β-CD:22-DHBP and 33-DHBP was weighed and transferred into a mortar. The mixture should be grained for 3 h, then transferred and stored in an airtight container.

2.7. Antibacterial studies

The antibacterial assay tested both gram-positive and gram-negative bacterial pathogens. E. coli (EC) and Staphylococcus aureus (SA) were used to represent the gram- negative and gram-positive bacteria. Three methods - kneading, solution, and physical - were used to prepare the complex for the study. The solid samples were dissolved in DMSO solvent in the concentration of 2 mg in 50 ml as stock solution. A few sterile Petri dishes were taken, and the nutrient agar medium was allowed, and

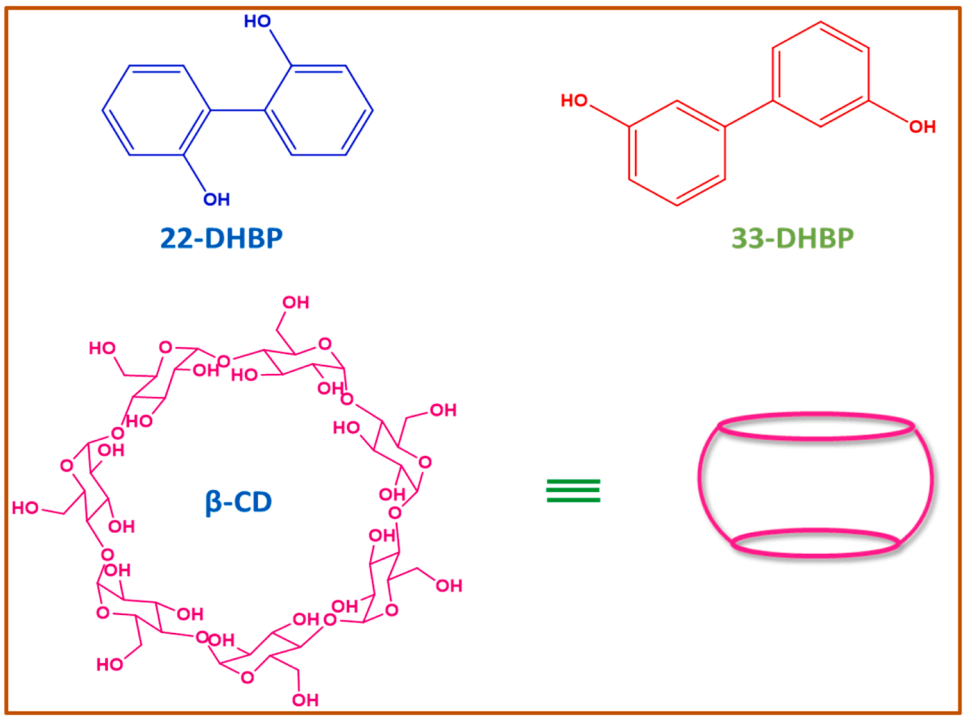

Scheme 1. Chemical structures of β-CD, 22-DHBP and 33-DHBP.

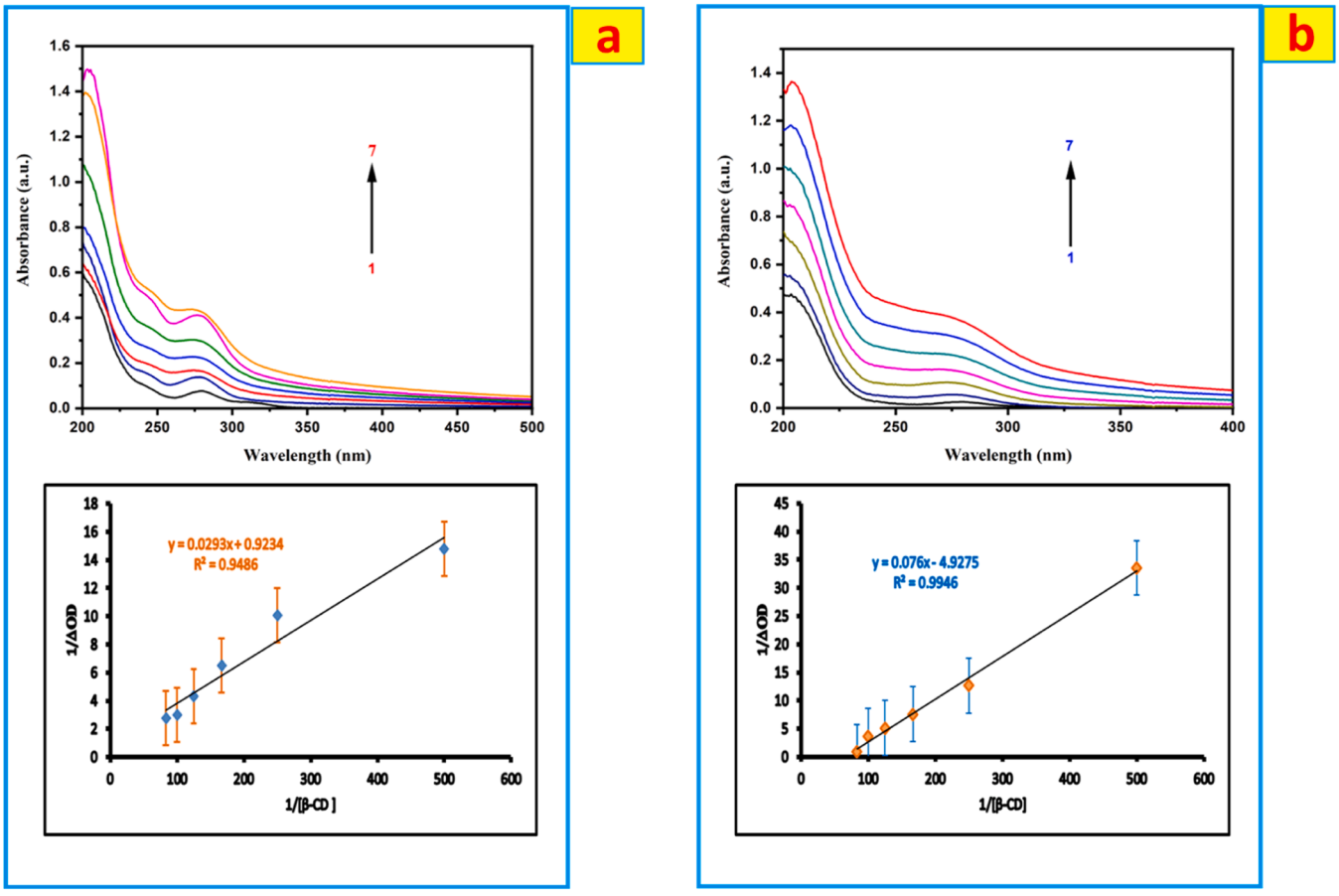

Fig. 1. UV–Visible absorption spectra and Benesi-Hildebrand plot of (a) 22-DHBP and (b) 33-DHBP (4×10^{-4} M) with various concentrations of β-CD (1) 0.0 M, (2) 0.002 M, (3) 0.004 M, (4)0.006 M, (5) 0.008 M, (6) 0.010 M and (7) 0.012 M.

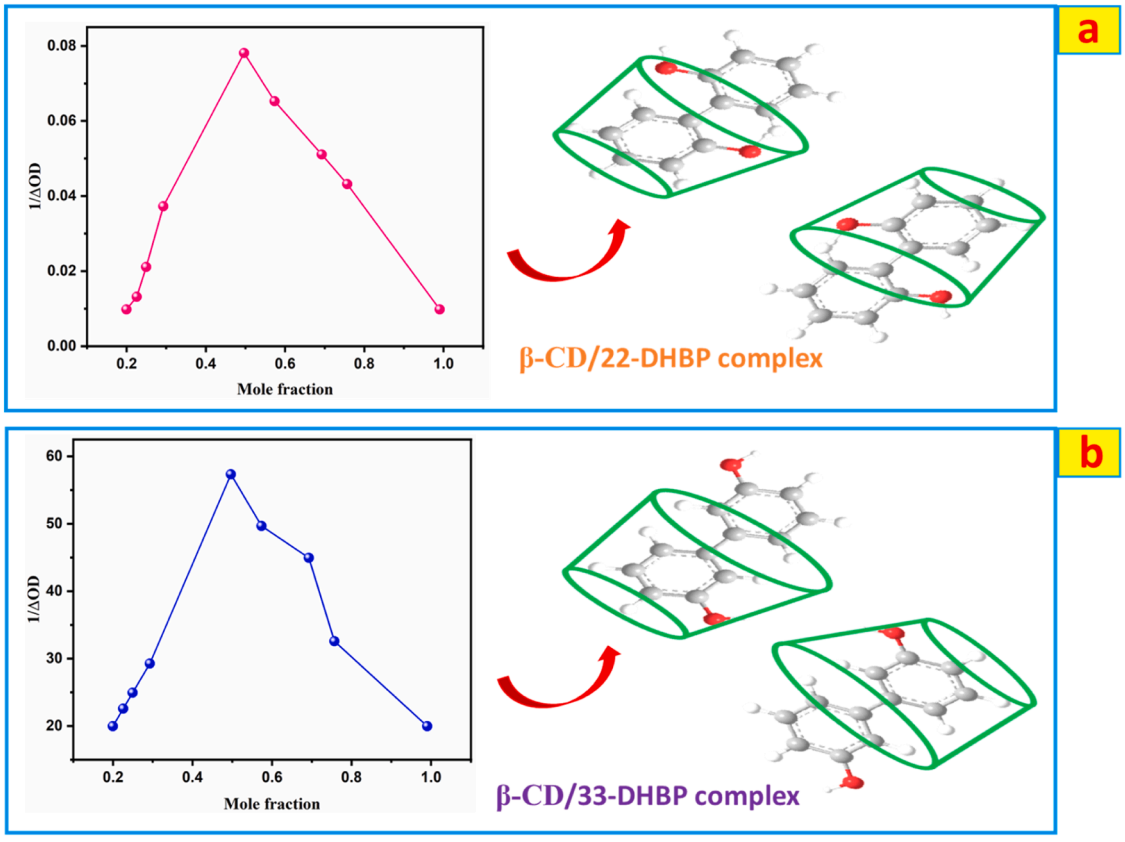

Fig. 2. Structure proposed from Jobs plot of β-CD inclusion complex with (a) 22-DHBP and (b) 33-DHBP.

solidify. Swipe the microbes (*E. coli* & *Staphylococcus aureus*) in the Petri dishes. This was kept in the incubator for five hours. Lawns of bacteria were grown all over the surface of the nutrient agar plates. Using a sterile gel puncher, five wells were made which are equidistant from each other. Three solid complexes, analyte, and β-CD of the same concentration, and same volume were added to the well and put in an incubator at 37 °C for 24 h. After 24 h the zone inhibition around the well was measured. All these were carried out in an aseptic condition.

3. Results and discussion

The chemical structures of β-CD, 22-DHBP, and 33-DHBP are given in Scheme 1. The host-guest binding between the guest and the host molecule could be assigned via intermolecular hydrogen bonding and pi-pi stacking interactions.

3.1. Absorption studies

The absorption maxima of 22-DHBP ($4 \times 10^{-}4$ mol dm^{-3}) at 276 nm is due to the π-π* transition of the benzene ring present. The absorption intensities increase with increasing β-CD concentration as detected shown in Fig. 1a. Changes in the intensity of absorption maxima 22-DHBP in the presence of β-CD describe the binding or inclusion complexation characteristics. The binding constant value gained from the Benesi-Hildebrand plot (Fig. 1a) is 3.1×10^{2} M^{-1}. The Job's plot shown in Fig. 2a, reveals 0.5 mole fraction proposes a 1:1 association ratio of 22-DHBP and β-CD.

33-DHBP ($2 \times 10^{-}5$ mol dm^{-3}) shows absorption maxima of 278 nm is attributed to the π-π* transition of the phenyl ring in water. In the presence of β-CD, there is a slight blue shift appeared from ~278 nm to ~275 nm, which shows a prominent complex formation. It has been observed that absorption intensities increase with increasing β-CD concentration as shown in Fig. 1b. This behavior has been attributed to the enhanced complex formation of the 33-DHBP through the hydrophobic interaction with β-CD [40]. These results indicate that the 33-DHBP molecule was entrapped into the β-CD cavity. The 1:1 inclusion complex of the guest and host is confirmed by Job's plot. In absorption spectra, the binding constant for the formation 3,3′-DHBP: β-cd complex has been determined by analyzing the changes in the intensity of absorption maxima with the β-CD concentration. The Benesi-Hildebrand plot is shown in Fig. 1b. The binding constant value obtained from the Benesi-Hildebrand plot is 6.4×10^{2} M^{-1} using Eqn (1).

3.2. Fluorescence studies

Initially, the 22-DHBP concentration was fixed at 4×10^{-4} M and the β-CD concentration varied from 1×10^{-3} M to 12×10^{-3} M, and the emission measurements proceeded. The emission maxima observed for 22-DHBP is at 399 nm, where the excitation wavelength is 280 nm. Fluorescence measurement is a highly sensitive technique than absorption measurement and also the β-CD does not possess fluorescence characteristics. This is an accurate method to investigate the binding interaction of 22-DHBP with β-CD. The emission intensity of 22-DHBP rises after increasing the concentration of β-CD (Fig. 3a), exhibiting the complexation behavior. The binding constant value is calculated from the changes in emission intensity of 22-DHBP, using modified Benesi-Hildebrand Eqn (2).. The binding constant value obtained is 8.12×10^{3} M^{-1}.

The fluorescence spectra of 33-DHBP in various concentrations of β-CD. This shows an isosbesitic point at 360 nm. There was a slight red shift experienced from ~376 nm to ~400 nm showing the complex formation in the exited state. The fluorescence intensity decreases at ~400 nm when the concentration of the β-CD increases shown in Fig. 3b. The decrease in emission intensity was due to static quenching in the exited state. The domination of a less polar environment experienced by the guest molecule in the cavity of the macromolecule and the small red

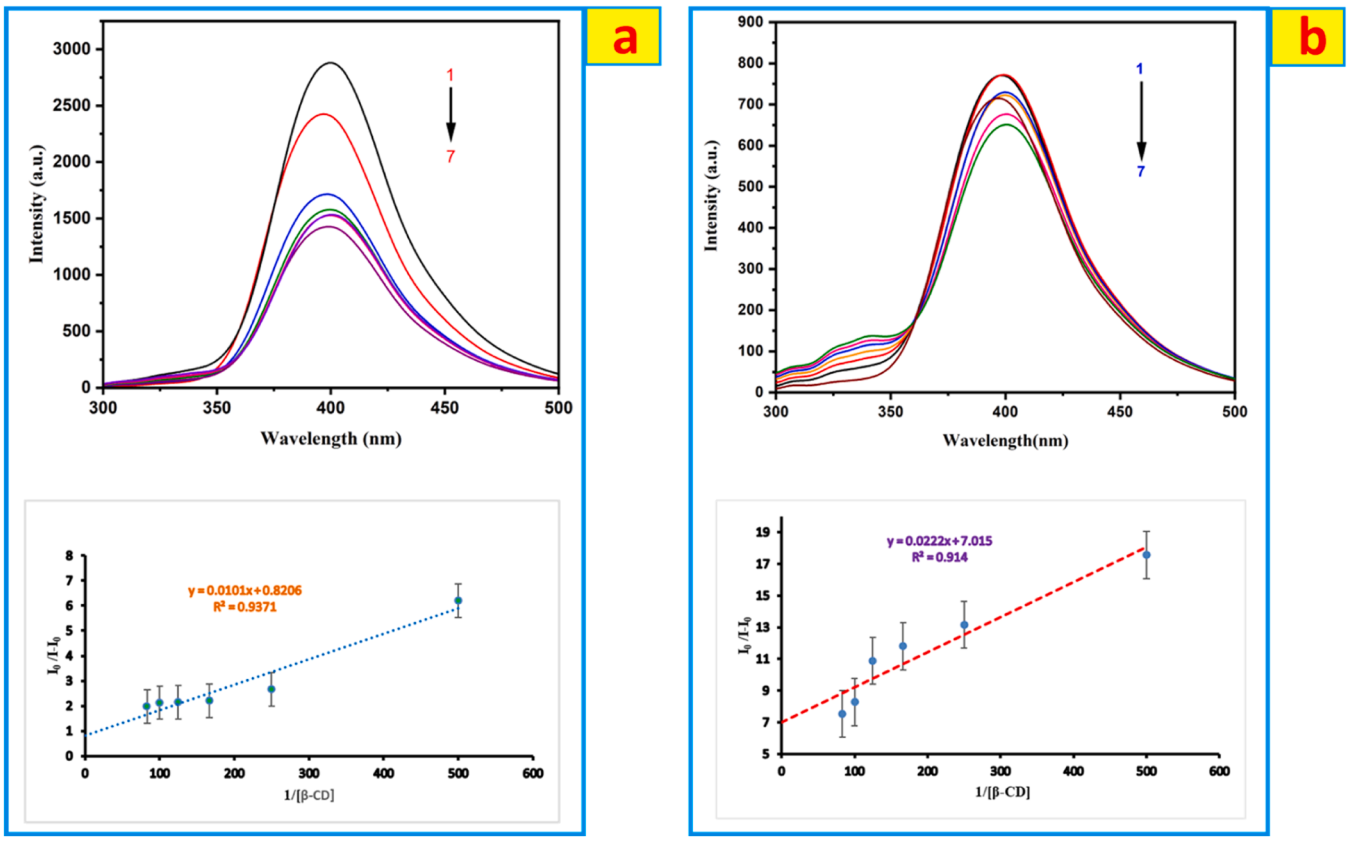

Fig. 3. Emission spectra and modified Benesi-Hildebrand plot of (a) 22-DHBP and (b) 33-DHBP (4×10^{-4} M) with various concentrations of β-CD (1) 0.0 M, (2) 0.002 M, (3) 0.004 M, (4)0.006 M, (5) 0.008 M, (6) 0.010 M and (7) 0.012 M.

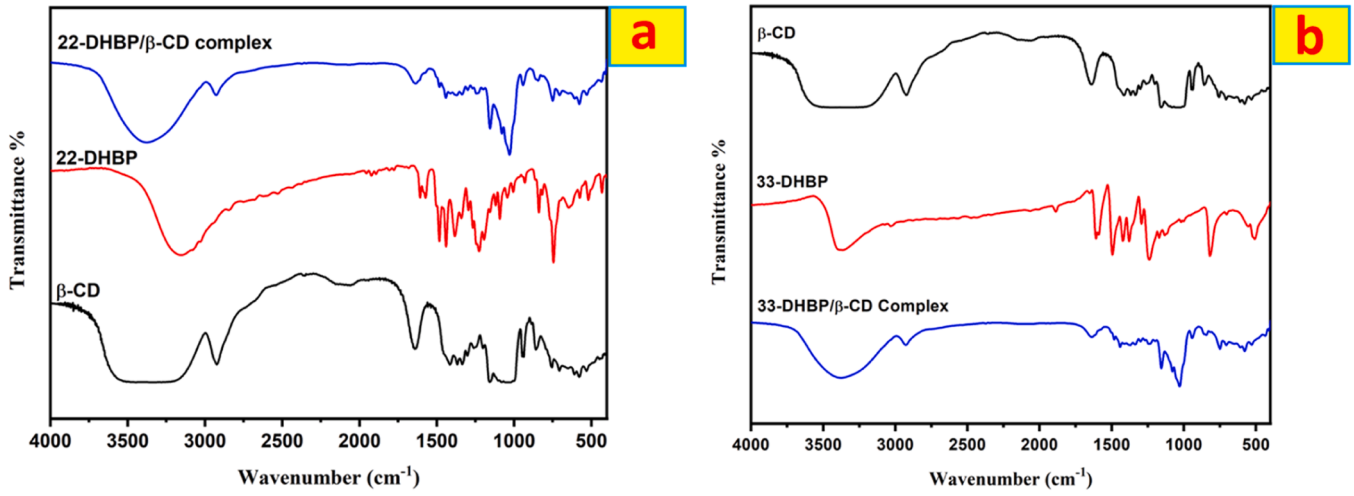

Fig. 4. FTIR spectra of prepared solid supramolecular complex (a) 22-DHBP/β-CD and (b) 33-DHBP/β-CD system.

emission is due to dipole-dipole interaction between the OH group of guest and host [11]. The binding constant value rescued is from the changes in emission intensity of 33-DHBP, using modified Stern-Volmer equation Eqn (2).. The binding constant value obtained is 3.15×10^3 M^{-1}.

3.3. FT-IR analysis

The FTIR spectra of 22-DHBP/β-CD and 33-DHBP/β-CD systems compared with free β-CD, 22-DHBP, and 33-DHBP molecules are shown in Fig. 4. The β-CD alone has its major stretching and bending vibrations of -OH, C—H, and C—O are discussed as follows. A broad absorption band is observed at the region of around 3500–3200 cm^{-1} corresponding to -OH stretching vibration. A sharp peak at 2925 cm^{-1} designates the asymmetric and symmetrical methylene -CH_2 vibrations. The major peaks at 1640 cm^{-1} and 1044 cm^{-1} represent the –C = C and C—O stretching vibrations [29,41]. The guest molecules 22-DHBP and 33-DHBP alone also have their own characteristics peaks of -OH stretching, aromatic C = C, and C—C are observed at around 3200–3400 cm^{-1}, 1600 cm^{-1}, and 1450 cm^{-1} vibrational frequencies. The FTIR spectra of 22-DHBP/β-CD and 33-DHBP/β-CD inclusion complex possess peak shifts and changes in intensity compared to free guest and host

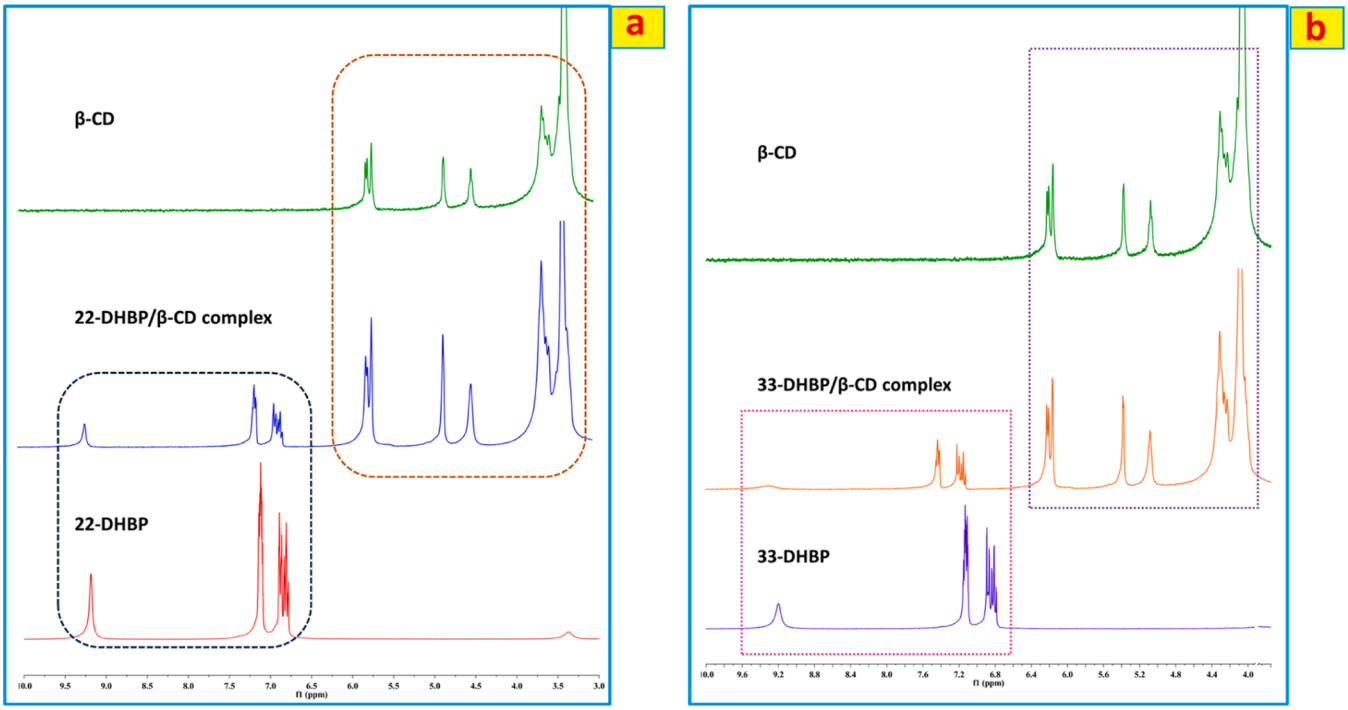

Fig. 5. ^{1}H NMR spectra of (a) 22-DHBP/β-CD and (b) 33-DHBP/β-CD system in D_2O.

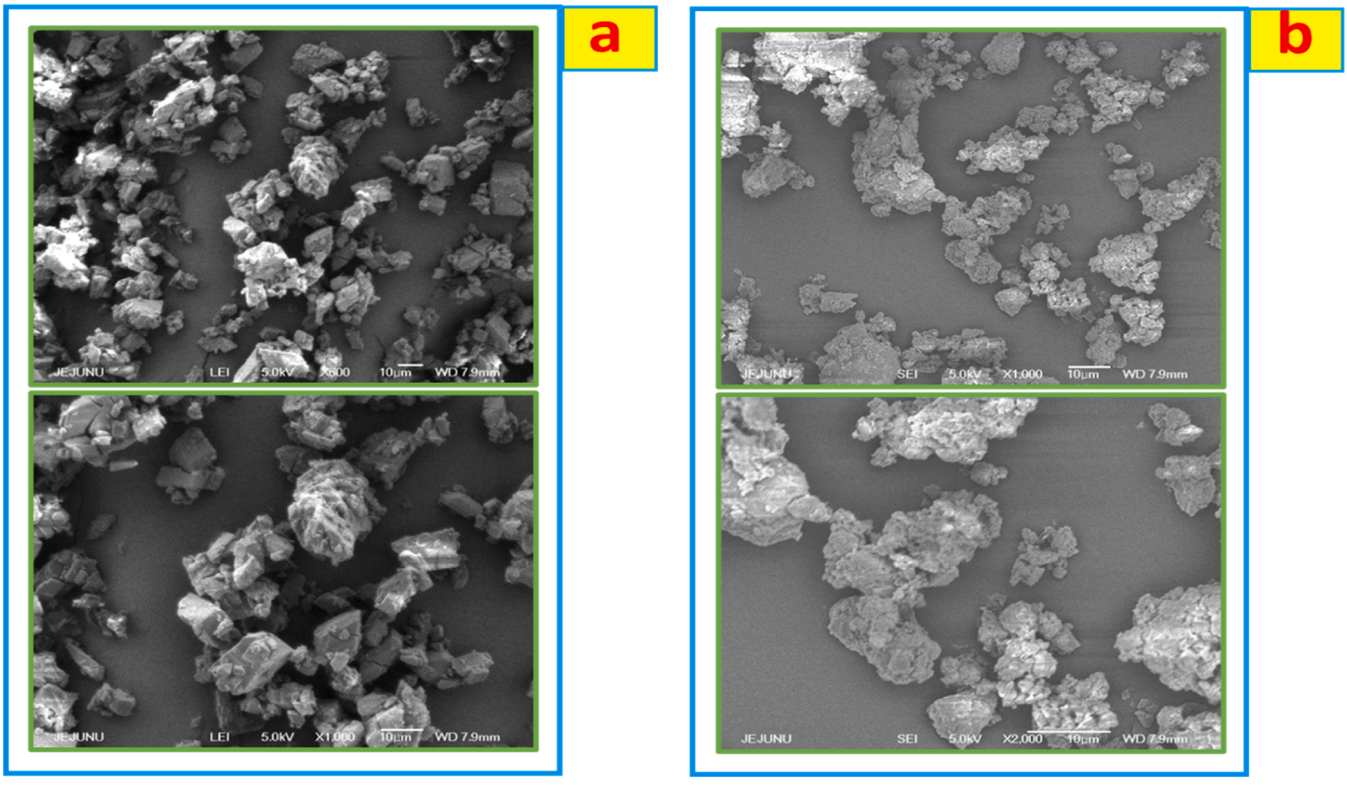

Fig. 6. SEM images solid inclusion complex of (a) 22-DHBP/β-CD and (b) 33-DHBP/β-CD system.

molecules. The hydrogen-bonded -OH groups appeared in the region of 3385 cm^{-1} of the obtained solid inclusion complex [24]. The aromatic C = C stretching vibration is observed at 1644 cm^{-1} of both the prepared solid complexes, which appeared at 1640 cm^{-1} for β-CD alone. A peak at 1030 cm^{-1} corresponds to the C—O stretching vibration of β-CD present in the inclusion complex [34].

3.4. NMR analysis

All the methylene, hydroxyl, and aromatic protons of β-CD appeared in the region of 3.2 ppm to 5.94 ppm as shown in Fig. 5. Hydroxyl protons of free 22-DHBP are observed at 9.18 ppm and the aromatic protons at the region of 6.7–7.14 ppm are shown in Fig 5a. All the

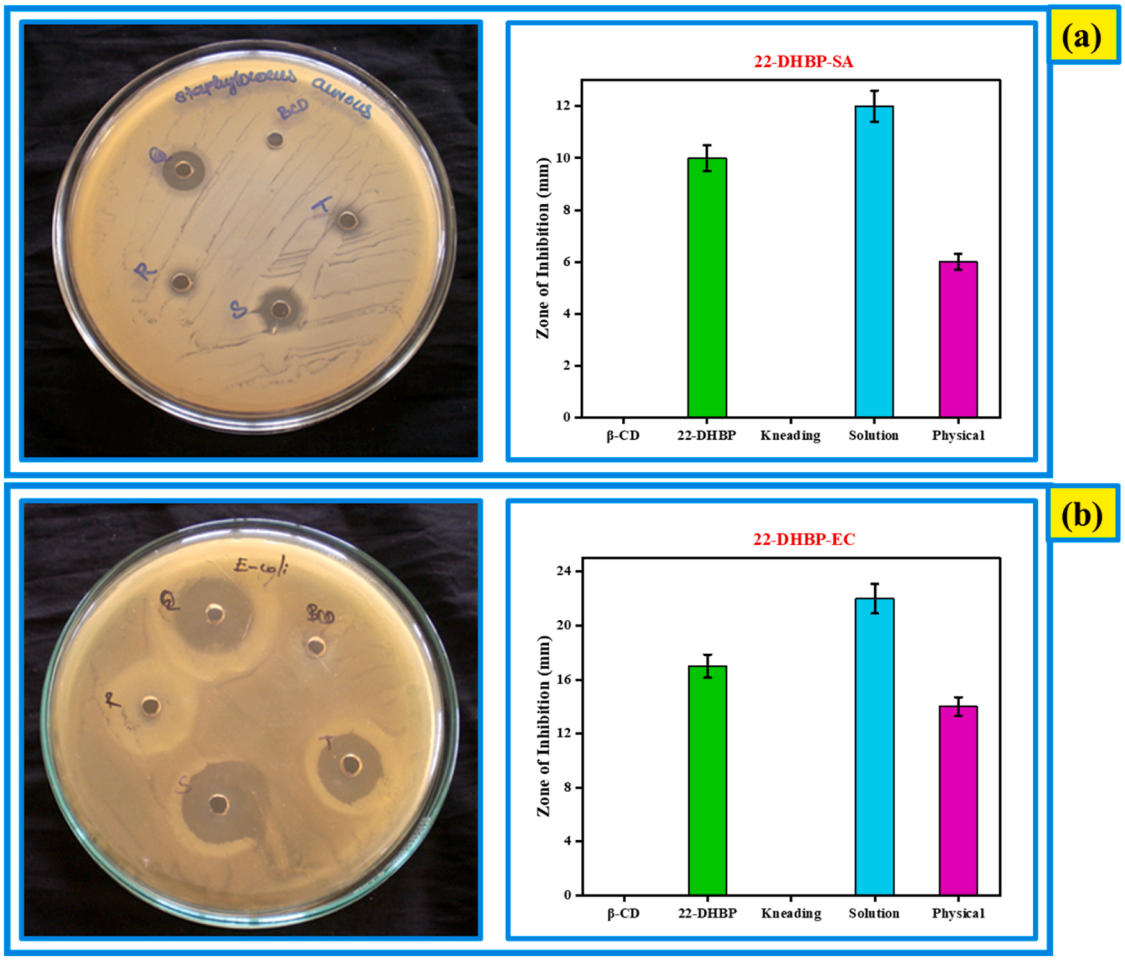

Fig. 7. The zone of inhibition and activity bar diagram of 22-DHBP/β-CD complex tested with microbes (a) Staphylococcus aureus and (b) Escherichia coli bacteria.

protons of 22-DHBP are shifted towards the downfield in the 22-DHBP/β-CD inclusion complex, expressed by the interaction of these protons with the β-CD [42]. The protons of β-CD have experienced the upfield shift for the inclusion complex, revealing the encapsulation of 22-DHBP inside the β-CD cavity.

Similarly, the 33-DHBP/β-CD supramolecular complex is examined by ^{1}H NMR spectroscopy (Fig. 5b). Protons of 33-DHBP appeared at the chemical shift values of 9.22 ppm (-OH protons) and 6.7–7.15 ppm are the protons of the aromatic phenyl ring. The 33-DHBP protons display a downfield shift for the prepared 33-DHBP/β-CD complex indicating the binding characteristics of 33-DHBP with β-CD. Also, the shift in the β-CD protons confirms the inclusion of complex formation. The chemical shift value changes are shown in

3.5. SEM analysis

The SEM micrographs of prepared solid inclusion complexes of 22-DHBP/β-CD and 33-DHBP/β-CD system is given in Fig. 6. The SEM images of the 22-DHBP/β-CD complex display randomly occupied irregularly shaped granules morphology. The SEM images of 33-DHBP/β-CD based solid complex exhibit the morphology of the collective arrangement of unevenly shaped scraps. The same irregularly shaped granule morphology was observed in the 22-DHBP/β-CD and 33-DHBP/β-CD samples prepared using both the kneading and physical mixture methods, as depicted in **Fig S1**.

3.6. TG analysis

The TG analysis was used to study the thermal stability of the compound. **Fig. S2a & b** β-CD shows the initial weight loss (0~10 %) at 120 °C the dehydration of hydroxyl molecule, the major weight loss (80 %) at 370 °C in which the glycosidic bond connecting the glucose molecules break down, and leading to the formation of smaller fragments of glucose then, at 370~500 the residual weight loss occurs by decomposition of the glucose small fragments. In **Fig. S2 (a)** 22-DHBP hydroxyl (-OH) group present ortho position has decomposed at 280 °C whereas in **Fig. S2 (b)** hydroxyl group (-OH) of the 33-DPBP present in the meta position decomposed at 260 °C which implies the -OH group present in the ortho position has stable intramolecular hydrogen bonding when compared to the 33-DHBP. Then, the β-CD/22-DHBP and β-CD/33-DHBP have a primary decomposition of hydroxy and volatile compounds (10 %) at 100 °C, and the partial decomposition of glycosidic bonds of the β-CD occurs at 250 °C. The major decomposition of β-CD encapsulated 22-DHBP occurs at 450 °C due to the breakdown of the biphenyl structure, whereas 33-DHBP encapsulated with β-CD has the major decomposition of 430 °C. So, from this TG analysis, the prepared 22-DHBP/ β-CD and 33-DHBP/ β-CD have withstood up to 450 and 430 °C.

3.7. Antibacterial activity

The observations using 22-DHBP/β-CD complex on gram-positive was shown in Fig. 7a. The figure clearly showed the complex prepared by the solution method shows significant antibacterial activity against

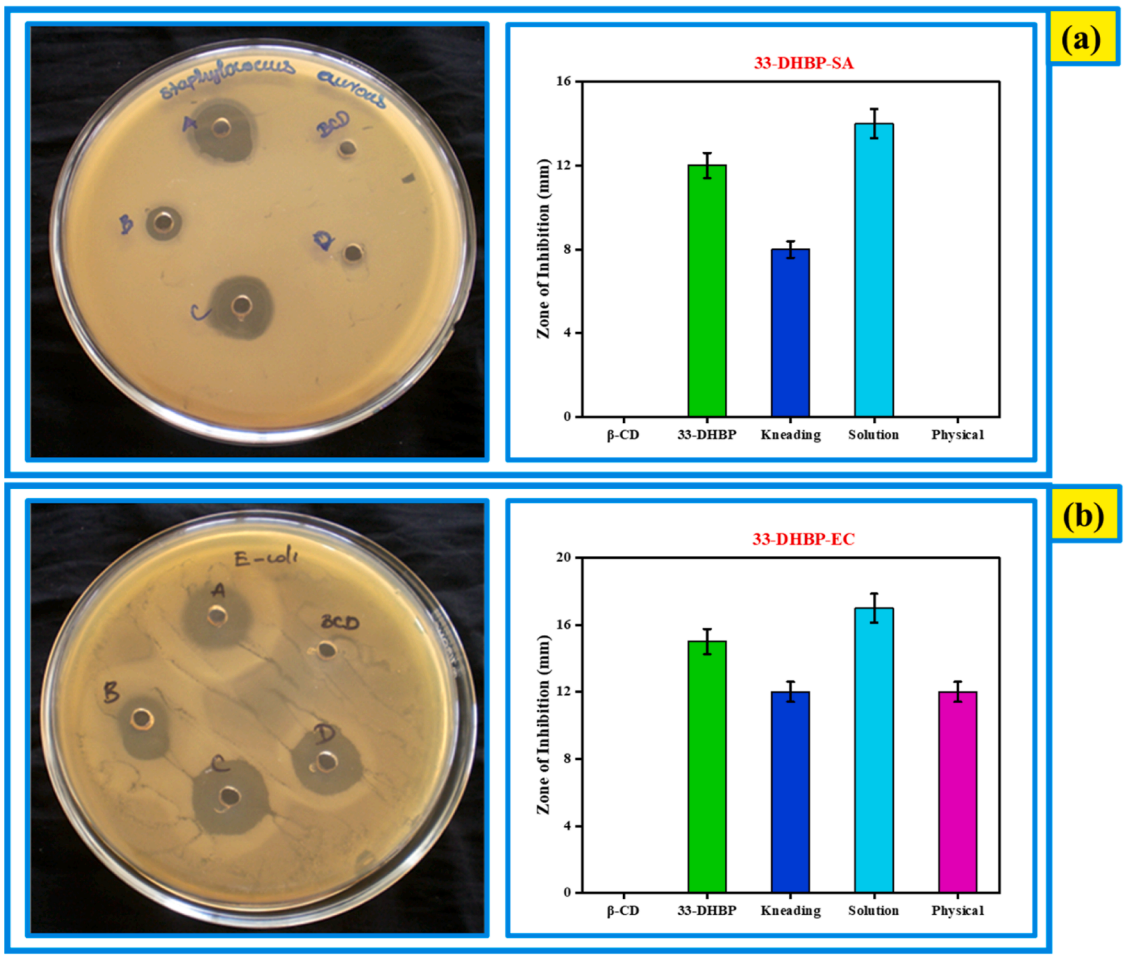

Fig. 8. The zone of inhibition and antibacterial activity of 33-DHBP/β-CD complex tested with bacteria (a) Staphylococcus aureus and (b) Escherichia coli bacteria.

the gram-positive bacteria, the complex formed by the physical method and the analyte shows moderate activity and others show very low or no activity on the pathogens. Whereas in gram-negative bacteria in Fig. 7**b**, the complexes prepared by solution show high activity the complexes prepared by physical method and the analyte show moderate activity, and others have very low or no activity.

The antibacterial studies using 33-DHBP and its complex on gram-positive was shown in Fig. 8a. The figure it was shows the complex prepared by the solution method shows leading antibacterial activity against the gram-positive bacteria, the complex obtained from the kneading method, and the analyte shows moderate activity and others show very low or no activity on the pathogens. The activity of gram-negative bacteria is given in Fig. 8b, the complexes prepared by solution show high activity and the complexes prepared by physical method, kneading method, and the analyte show moderate activity and others have very low or no activity.

Fig. S3 shows the efficiency of the 22-DHBP, 33-DHBP, and inclusion complexes prepared by the kneading, solution, and physical method, compared with the standard (amikacin) zone of inhibition of about 16 (mm). The efficiency was calculated using the formula in Eq. (3).

$$\frac{Zone\ of\ inhibiton\ (Compound)}{Zone\ of\ inhibiton\ (Control)} \times 100 \qquad (3)$$

From **Fig. S3(a)** calculation, the β-CD,22-DHBP, inclusion compound prepared by kneading, solution, and physical methods has an efficiency of 0 %, 62.5 %, 0 %, 75 %, and 37.5 % respectively, and in **Fig. S3(b)**, the β-CD,33-DHBP, inclusion compound prepared by kneading, solution, and physical methods has an efficiency of 0 %, 75 %, 50 %, 87.5 %, and 0 % respectively. In both the inclusion complexes of 22-DHBP and 33-DHBP, the inclusion complex prepared by the solution method has a leading efficiency, and Zone of inhibition compared to the rest of the methods, which is strong evidence that the material can be used in treating bacterial cells (antibacterial activity) (Table 1).

Table 1
Changes in the chemical shift values of 22-DHBP and 33-DHBP guests in the presence of β-CD host.

Protons	Chemical Shifts (ppm)			
	22-DHBP	22-DHBP/β-CD complex	33-DHBP	33-DHBP/β-CD complex
OH	9.18	9.2	9.	9.21
Aromatic	7.12	7.15	7.13	7.17
	6.78–6.89 (multiplets)	6.78–6.91 (multiplets)	6.78–6.88 (multiplets)	6.78–6.90 (multiplets)

3.8. Plausible mechanism for the antibacterial action of DHBP/β-CD complex in the bacteria cell

Compounds such as 22-DHBP and 33-DHBP have moderate antibacterial activity against bacteria in such cases on inclusion with cyclodextrins that enhance the solubility of the 22-DHBP and 33-DHBP which can easily penetrate the hydrophilic part of the bacterial membrane and interact with the key enzymes which are responsible for the primary function of the bacterial cell to lose its fluid content (cell lysis) and causes the bacterial cell death that shown in Fig. 9.

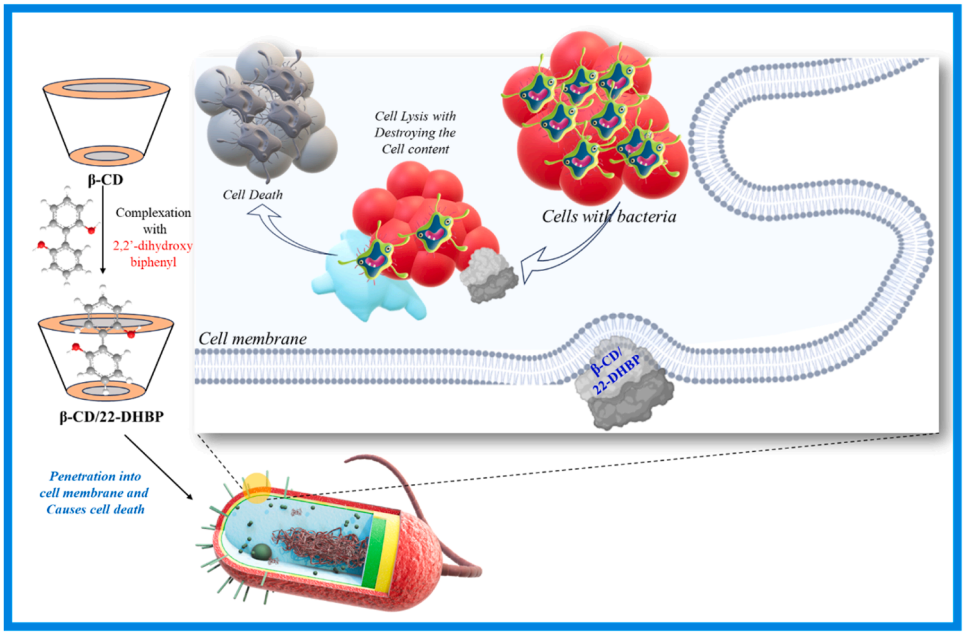

Fig. 9. Schematic diagram of antibacterial action of DHBP/β-CD complex in the bacteria cell.

4. Conclusion

In summary, the inclusion complexation study is a potential strategy for improving the antibacterial activity of 22-DHBP and 33-DHBP molecules. The binding study on 22-DHBP and 33-DHBP with β-CD host using the UV absorption, and fluorescence other studies on solid complexes were interpreted. The absorption spectra of the guest molecules were recorded with various concentrations of β-CD. Enhancement in the absorbance intensity with increasing concentration of β-CD explores the binding characteristics. The Job's plot exhibits a 1:1 stochiometric ratio of binding of guests with the β-CD host from the absorption titrations. The emission titration also reveals clear support for the binding of β-CD with guest molecules through quenching of emission intensity. The binding constant value of 22-DHBP is 8.12×10^3 M^{-1}, and 33-DHBP is 3.15×10^3 M^{-1}. The results conclude that the β-CD can enhance the solubility of the 22-DHBP and 33-DHBP molecules with the help of inclusion processes. The prepared solid inclusion complex shows the characteristic stretching and bending vibrations in both the guests (22-DHBP & 33-DHBP) and the β-CD host. In the ^{1H}NMR spectra, the inclusion complex shows some downfield shifting of guest molecule protons upon binding. The protons of β-CD display up field shift, describing the cavity as occupied with the guest molecules. The SEM images of the solid complex obtained from both the guest molecules possess randomly occupied irregularly shaped granules morphology. The complex prepared by solution method shows leading antibacterial activity against the gram-positive and gram-negative bacteria than the kneading method and the physically mixed one.

CRediT authorship contribution statement

Kumaraswamy Paramasivaganesh: Writing – original draft, Methodology, Formal analysis, Conceptualization. **Chandramohan Govindasamy:** Resources, Project administration, Funding acquisition. **Esakkimuthu Shanmugasundaram:** Formal analysis, Validation. **Nithesh Kumar Krishnan:** Data curation, Resources. **Chokalingam Saravanan:** Formal analysis, Data curation. **Jayaraman Thanusu:** Resources, Validation, Visualization. **Stalin Thambusamy:** Writing – review & editing, Writing – original draft, Supervision, Conceptualization.

Declaration of competing interest

The authors confirm that they have no known financial or interpersonal conflicts that would have appeared to have an impact on the research presented in this study. As the manuscript's authors, none of us have any competing interests in the work at hand. I have put my signature on this and forwarded it to your respected journal for consideration of publishing on behalf of all the authors who have indicated their involvement and have contributed to the writing of this article.

Data availability

Data will be made available on request.

Ethical approval

No humans or animals have been used in this research.

Availability of data and materials

The datasets used or analyzed during the current study are available from the corresponding author upon reasonable request.

Notes

The authors declare no competing financial interest.

Acknowledgment

This project was supported by Researchers Supporting Project number (RSPD2024R712), King Saud University, Riyadh, Saudi Arabia.

Author information

Corresponding Author
ORCID: 0000–0002–0400–4274.

Supplementary materials

Supplementary material associated with this article can be found, in the online version, at doi:10.1016/j.molstruc.2024.139701.

References

[1] A. Cid-Samamed, J. Rakmai, J.C. Mejuto, J. Simal-Gandara, G. Astray, Cyclodextrins inclusion complex: Preparation methods, analytical techniques and food industry applications, Food Chem. 384 (2022) 132467.
[2] M. Banchero, Supercritical carbon dioxide as a green alternative to achieve drug complexation with cyclodextrins, Pharmaceuticals 14 (2021).
[3] J. Chen, X. Qin, S. Zhong, S. Chen, W. Su, Y. Liu, Characterization of curcumin/cyclodextrin polymer inclusion complex and investigation on its antioxidant and antiproliferative activities, Molecules. 23 (2018).
[4] J.J. Li, Y. Chen, H.Y. Zhang, X. Dai, Y. Liu, Application of Macrocycle-Based Supramolecular Assemblies Based on Aggregation-Induced Emission, Handb. Macrocycl. Supramol. Assem. With 1098 (2020) 1345–1368.
[5] Q.Q. Wang, Supramolecular Catalysis Using Organic Macrocycles, 2019.
[6] Z. Yang, H. Tang, Y. Liu, Spectroscopy Studies of Macrocyclic Supramolecular.
[7] M. Rudrapal, T. Babu, T. Chandra, U. Durga, V. Swathi, B. Chandrika, K. Ravishankar, Synthesis and Evaluation of Heterocyclic Scaffold-Based Styrene Conjugates as New Antibacterial Agents, Antiinfect. Agents 12 (2014) 198–205.
[8] S. Pandey, V.K. Soni, G. Choudhary, P.R. Sharma, R.K. Sharma, Understanding behaviour of vitamin-C guest binding with the cucurbit [6]uril host, Supramol. Chem. 29 (2017) 387–394.
[9] R.V. Rodik, A.S. Klymchenko, Y. Mely, V.I. Kalchenko, Calixarenes and related macrocycles as gene delivery vehicles, J. Incl. Phenom. Macrocycl. Chem. 80 (2014) 189–200.
[10] Z. Zeng, Y. Zhang, X. Zhang, G. Luo, J. Xie, Z. Tao, Q. Zhang, Selective detection of Zn2+ and Cd2+ ions in water using a host-guest complex between chromone and Q [7], Chinese Chem. Lett. 32 (2021) 2572–2576.
[11] M. Sayed, H. Pal, An overview from simple host-guest systems to progressively complex supramolecular assemblies, Phys. Chem. Chem. Phys. 23 (2021) 26085–26107.
[12] J. Yu, D. Qi, J. Li, Design, synthesis and applications of responsive macrocycles, Commun. Chem. 3 (2020) 1–14.
[13] M.A. Esteso, C.M. Romero, Cyclodextrins: Properties and Applications, Int. J. Mol. Sci. 25 (2024) 1–5.
[14] M. Sonaimuthu, S.B. Balakrishnan, S.V. Kuppu, G.B. Veerakanellore, S. Thambusamy, Spectral and proton transfer behavior of 1,4-dihydroxylanthraquinone in aqueous and confined media; molecular modelling strategy, J. Mol. Liq. 259 (2018) 186–198.
[15] F. Maest, M. Jos, H.B. Firmino, J. Gabriella, R. De Cassia, S. Curto, A. Borges, F. Alexandre, P. Scacchetti, L. Tessaro, The Role of β -Cyclodextrin in the Textile Industry — Review, Molecules. 25 (2020) 3624.
[16] K. Sarkar, B.K. Barman, M.Nath Roy, Study to explore inclusion complexes of A- and B-cyclodextrin molecules with 3-octyl-1-methylimidazolium bromide with the manifestation of hydrophobic and hydrophilic interactions, Chem. Phys. Lett. 707 (2018) 13–21.
[17] M.N. Roy, D. Ekka, S. Saha, M.C. Roy, Host-Guest Inclusion Complexes of α and β -Cylodextrins with α -Amino Acids 80 (2014) 42383–42390.
[18] R. Paul, S. Paul, Synergistic host-guest hydrophobic and hydrogen bonding interactions in the complexation between endo-functionalized molecular tube and strongly hydrophilic guest molecules in aqueous solution, Phys. Chem. Chem. Phys. 20 (2018) 16540–16550.
[19] Z.I. Szabó, R. Deme, Z. Mucsi, A. Rusu, A.D. Mare, B. Fiser, F. Toma, E. Sipos, G. Tóth, Equilibrium, structural and antibacterial characterization of moxifloxacin-β-cyclodextrin complex, J. Mol. Struct. 1166 (2018) 228–236.
[20] M. Liu, P. Lv, R. Liao, Y. Zhao, B. Yang, Synthesis, characterization and biological activity of Rhein-cyclodextrin conjugate, J. Mol. Struct. 1128 (2017) 239–244.
[21] S. Saha, A. Roy, K. Roy, M.N. Roy, Study to explore the mechanism to form inclusion complexes of β-cyclodextrin with vitamin molecules, Sci. Rep. 6 (2016) 1–12.
[22] A. Celebioglu, T. Uyar, Metronidazole/Hydroxypropyl-β-Cyclodextrin inclusion complex nanofibrous webs as fast-dissolving oral drug delivery system, Int. J. Pharm. 572 (2019) 118828.
[23] C. Dong, L.Y. Qian, G.L. Zhao, B.H. He, H.N. Xiao, Preparation of antimicrobial cellulose fibers by grafting β-cyclodextrin and inclusion with antibiotics, Mater. Lett. 124 (2014) 181–183.
[24] S. Mohandoss, S. Palanisamy, S.G. You, J.J. Shim, Y.Rok Lee, Ultrasonication-assisted host–guest inclusion complexes of β-cyclodextrins and 5-hydroxytryptophan: Enhancement of water solubility, thermal stability, and in vitro anticancer activity, J. Mol. Liq. 336 (2021) 116172.
[25] S. Goswami, M. Sarkar, Fluorescence, FTIR and 1H NMR studies of the inclusion complexes of the painkiller lornoxicam with β-, γ-cyclodextrins and their hydroxy propyl derivatives in aqueous solutions at different pHs and in the solid state, New J. Chem. 42 (2018) 15146–15156.
[26] C.S. Marques, S.G. Carvalho, L.D. Bertoli, J.C.O. Villanova, P.F. Pinheiro, D.C. M. dos Santos, M.I. Yoshida, J.C.C. de Freitas, D.F. Cipriano, P.C. Bernardes, β-Cyclodextrin inclusion complexes with essential oils: Obtention, characterization, antimicrobial activity and potential application for food preservative sachets, Food Res. Int. 119 (2019) 499–509.
[27] A. Celebioglu, T. Uyar, Development of ferulic acid/cyclodextrin inclusion complex nanofibers for fast-dissolving drug delivery system, Int. J. Pharm. 584 (2020) 119395.
[28] V. Jahed, A. Zarrabi, A.K. Bordbar, M.S. Hafezi, NMR (1H, ROESY) spectroscopic and molecular modelling investigations of supramolecular complex of β-cyclodextrin and curcumin, Food Chem. 165 (2014) 241–246.
[29] P. Tang, S. Li, L. Wang, H. Yang, J. Yan, H. Li, Inclusion complexes of chlorzoxazone with β- And hydroxypropyl-β-cyclodextrin: Characterization, dissolution, and cytotoxicity, Carbohydr. Polym. 131 (2015) 297–305.
[30] M. Chatzidaki, I. Kostopoulou, C. Kourtesi, I. Pitterou, S. Avramiotis, A. Xenakis, A. Detsi, β-Cyclodextrin as carrier of novel antioxidants: A structural and efficacy study, Colloids Surfaces A Physicochem. Eng. Asp. 603 (2020) 125262.
[31] K. Srinivasan, T. Stalin, Studies on inclusion complexes of 2,4-dinitrophenol, 2,4-dinitroaniline, 2,6-dinitroaniline and 2,4-dinitrobenzoic acid incorporated with β-cyclodextrin used for a novel UV absorber for ballpoint pen ink, J. Incl. Phenom. Macrocycl. Chem. 78 (2014) 337–350.
[32] K. Srinivasan, S. Radhakrishnan, T. Stalin, Inclusion complexes of β-cyclodextrin-dinitrocompounds as UV absorber for ballpoint pen ink, Spectrochim. Acta - Part A Mol. Biomol. Spectrosc. 129 (2014) 551–564.
[33] S. Mohandoss, M. Maniyazagan, T. Stalin, A highly selective dual mode detection of Fe^{3+} ion sensing based on 1,5-dihydroxyanthraquinone in the presence of β-cyclodextrin, Mater. Sci. Eng. C 48 (2015) 94–102.
[34] M.A. Chouker, H. Abdallah, A. Zeiz, M.H. El-Dakdouki, Host-quest inclusion complex of quinoxaline-1,4-dioxide derivative with 2-hydroxypropyl-β-cyclodextrin: Preparation, characterization, and antibacterial activity, J. Mol. Struct. 1235 (2021) 130273.
[35] D. Boczar, K. Michalska, Cyclodextrin Inclusion Complexes with Antibiotics and Antibacterial Agents as Drug-Delivery Systems—A Pharmaceutical Perspective, Pharmaceutics. 14 (2022) 14071389.
[36] M. Sondossi, D. Barriault, M. Sylvestre, Metabolism of 2,2′- and 3,3′-Dihydroxybiphenyl by the Biphenyl Catabolic Pathway of Comamonas testosteroni B-356, Appl. Environ. Microbiol. 70 (2004) 174–181.
[37] M. Rudrapal, D. Chetia, A. Prakash, Synthesis, antimalarial-, and antibacterial activity evaluation of some new 4-aminoquinoline derivatives, Med. Chem. Res. 22 (2013) 3703–3711.
[38] I.M.M. Othman, M.H. Mahross, M.A.M. Gad-Elkareem, M. Rudrapal, N. Gogoi, D. Chetia, K. Aouadi, M. Snoussi, A. Kadri, Toward a treatment of antibacterial and antifungal infections: Design, synthesis and in vitro activity of novel arylhydrazothiazolylsulfonamides analogues and their insight of DFT, docking and molecular dynamic simulations, J. Mol. Struct. 1243 (2021) 130862.
[39] E.S. Material, R.S.C. Advances, T.R. Society, 2 S1 Modified Stern – Volmer equation 8 S2 Double logarithm equation 13 S3 Van, t Hoff equation and thermodynamic equation 17 S4 The species of Hg (II) in the experimental system 10 (2015) 13–15.
[40] F. D'Aria, B. Pagano, C. Giancola, Thermodynamic properties of hydroxypropyl-β-cyclodextrin/guest interaction: a survey of recent studies, J. Therm. Anal. Calorim. 147 (2022) 4889–4897.
[41] S. Mohandoss, R. Atchudan, T.N.J. Immanuel Edison, T.K. Mandal, S. Palanisamy, S.G. You, A.A. Napoleon, J.J. Shim, Y.R. Lee, Enhanced solubility of guanosine by inclusion complexes with cyclodextrin derivatives: Preparation, characterization, and evaluation, Carbohydr. Polym. 224 (2019) 115166.
[42] A. Paulidou, D. Maffeo, K. Yannakopoulou, I.M. Mavridis, Crystal structure of the inclusion complex of the antibacterial agent triclosan with cyclomaltoheptaose and NMR study of its molecular encapsulation in positively and negatively charged cyclomaltoheptaose derivatives, Carbohydr. Res. 343 (2008) 2634–2640, ss.